

Characterization of mechanical properties of a hollow cylinder with zero group velocity Lamb modes

M. Cès, D. Royer, and C. Prada^{a)}

Institut Langevin-Ondes et Images, ESPCI ParisTech, CNRS UMR 7587, Université Paris Diderot, 10 rue Vauquelin, 75231 Paris Cedex 05, France

(Received 27 January 2012; revised 26 April 2012; accepted 15 May 2012)

Hollow cylinders used in the industry must be regularly inspected. Elastic guided waves, similar to Lamb modes in a plate, can propagate in the axial direction or around the circumference. They are sensitive to geometrical and mechanical parameters of the cylindrical shell. The objective of this paper is to show that zero group velocity (ZGV) Lamb modes can be used to bring out anisotropy and to measure elastic constants of the material. This study provides experimental and numerical investigations on a Zirconium alloy tube extensively used by the nuclear industry in reactor core components. A non-contact method, based on laser ultrasound techniques and ZGV Lamb modes, demonstrates that the difference observed between axial and circumferential guided waves cannot be explained by an isotropic model. Then, a transverse isotropic model is used for the Zircaloy tube. Four of the five elastic constants are directly extracted from ZGV resonance frequencies. The last one is deduced from the measured dispersion spectra. With this complete set of constants, a good agreement is obtained between theoretical and experimental dispersion curves for both axially and circumferentially propagating guided waves. © 2012 Acoustical Society of America. [http://dx.doi.org/10.1121/1.4726033]

PACS number(s): 43.40.Ey, 43.20.Mv, 43.35.Cg, 43.35.Yb [JDM]

Pages: 180–185

I. INTRODUCTION

A great variety of hollow cylinders are used in the industry as pipes for gases or liquids (water, oil, chemicals). Their geometrical and mechanical properties are parameters of importance for the structure integrity. For example, wall thickness variations (increased by deposits or decreased by corrosion) can cause damage (reduction of flow rate or leakage). In nuclear industry, material properties of Zircaloy cladding tubes need to be evaluated to ascertain of their safety and reliability.^{1,2}

The most popular methods used in nondestructive evaluation (NDE) are radiography, eddy current, and ultrasound techniques. Over the last decades, many NDE ultrasonic methods have been developed.³ For example, Lamb waves have been used for defect detection in pipe-lines.⁴ Compared with bulk acoustic waves, the guided waves are more suitable for long-range inspection of thin hollow cylinders. In this case, axially and circumferentially propagating guided waves must be distinguished.⁵ Conventional ultrasonic requires a coupling medium (liquid, gel, or rubber) for allowing the transmission of the ultrasound into the piece under test.⁶ Non-contact techniques using EMAT⁷ or air-coupled transducers⁸ have been investigated. Laser based ultrasonic (LBU) techniques eliminate coupling issues in the generation and detection of the elastic waves and have the potential for fast scanning. Usually, elastic waves are generated by a (pulsed) laser and detected by an (interferometric) optical probe.⁹ Sources of various shapes and particularly of small dimensions are available. The duration of the laser

pulse can be short and the acoustic waves excited can be detected locally, even if the surface is curved. Moreover, the emission and detection bandwidths can be larger than 20 MHz, thereby providing high spatial and temporal resolutions. It has been shown that LBU is an efficient tool for studying the dispersive propagation of Lamb modes and that material properties can be extracted from the measured dispersion spectrum.¹⁰

Recently, Yeh and Yang reported on a procedure based on a laser ultrasound technique for the characterization of mechanical properties of a Zircaloy tube.¹¹ Assuming the material is isotropic, they used the simplex algorithm to extract mechanical properties from dispersion spectra of guided waves. They found that the estimated Poisson's ratio depends significantly on the propagation direction. We infer from this result that the difference between axial and circumferential dispersion curves should not be caused by the cylindrical geometry but by the anisotropy of the material.

The anisotropy of metallic laminated plates can be measured using linearly polarized EMAT and shear thickness resonances.¹² The method proposed here is different as it exploits the local resonances of the structure that appear at frequencies where the group velocities of some Lamb modes vanish. At these particular points of their dispersion curves, the acoustical energy of the corresponding zero group velocity (ZGV) modes is trapped in the source area without any transfer to the adjacent plate medium.¹³ It has been shown that the resulting resonance is sensitive to local mechanical properties of isotropic¹⁴ and anisotropic¹⁵ materials.

The objective of this paper is to show that these ZGV modes can be used to bring out material anisotropy and to measure elastic constants of a Zirconium alloy. This article is organized as follows: In Sec. II, the main properties of

^{a)}Author to whom correspondence should be addressed. Electronic mail: claire.prada@espci.fr

ZGV Lamb modes are briefly exposed and the influence of the shell curvature on ZGV resonance frequencies is investigated. In Sec. III, the laser ultrasonic technique is presented and the results of ZGV resonance measurements are discussed in terms of material anisotropy. In Sec. IV, the transverse isotropic model is introduced. In Sec. V, the five elastic constants are extracted from ZGV resonances and dispersion spectra of axial and circumferential guided waves.

II. ZGV LAMB MODES

The propagation of Lamb waves (frequency f , wavelength λ) is represented by a set of dispersion curves in the angular frequency ($\omega = 2\pi f$) and wave number ($k = 2\pi/\lambda$) plane.¹⁶ In a free isotropic elastic plate, characterized by longitudinal and transverse bulk wave velocities V_L and V_T , symmetric (S_n) and antisymmetric (A_n) modes satisfy two independent characteristic equations. Using dimensionless quantities: $fd/V_T = \omega d/2\pi V_T$ and $d/\lambda = kd/2\pi$, Lamb wave frequency spectra only depend on one material parameter: The bulk wave velocity ratio V_L/V_T or the Poisson ratio ν .¹⁷

As shown in Fig. 1 (dashed line), plotted for $\nu = 0.34$, A_0 and S_0 modes exhibit free propagation to zero frequency whereas higher order modes admit a cut-off frequency f_c when the wave number k approaches zero. Some branches of the dispersion curves $\omega(k)$ exhibit minima for non-zero wave numbers. At the corresponding points, the group velocity $d\omega/dk$ vanishes, whereas the phase velocity ω/k remains finite. For example, the first order symmetric (S_1) mode exists for small wave numbers at frequencies below the transverse cut-off frequency $f_c = V_T/d$. The frequency decays from $k = 0$ down to a minimum. At the minimum frequency of the S_1 -Lamb mode, which corresponds to the junction of S_1 and S_{2b} branches, a very sharp resonance can be observed.¹⁸ The S_1S_2 ZGV resonance frequency is proportional to the longitudinal cut-off frequency $f_c = V_L/2d$, reached for $k = 0$.

In fact, other ZGV Lamb modes exist. The range of existence of these symmetric or antisymmetric ZGV modes and their frequency depend on Poisson's ratio ν .¹⁹ Clorennec

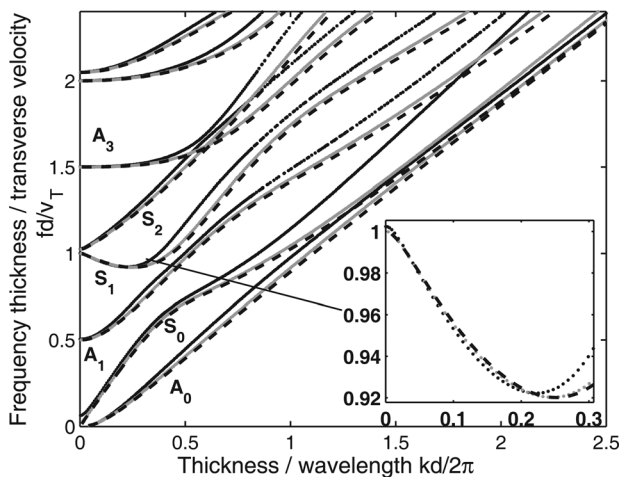


FIG. 1. Dispersion curves calculated for a material of Poisson ratio $\nu = 0.34$ for Lamb modes in a plate of thickness d (dashed black line) and circumferential guided waves in a hollow cylinder of external radius $b = 5d$ (black points) and $b = 21d$ (gray points).

et al. proved that the values of the resonance frequency obtained for the first two ZGV modes provided the local value of ν and either the plate thickness d if the longitudinal and transverse velocities were known or the bulk wave velocities if the plate thickness was known.¹⁴ At the thickness resonance ($k=0$), the whole surface is vibrating in phase. Conversely, with a finite wave number, ZGV modes give rise to local resonances, having a lateral extension of about twice the plate thickness. Thus a specific advantage of such measurements is the locality of the result.

As elastic waves guided by the shell of a hollow cylinder are similar to Lamb waves, ZGV modes also exist on cylindrical surfaces.¹⁴ A numerical study has been performed with the *Disperse* software²⁰ to assess the influence of curvature on ZGV resonance frequencies. The dispersion curves of circumferential and axial guided waves were calculated for a material of Poisson's ratio $\nu = 0.34$ for different ratios between the external radius b and the shell thickness d . As shown in Fig. 1 for circumferential waves, the curvature induces significant changes in particular for the A_0 and S_0 modes. However, for both axial and circumferential modes the ZGV and thickness frequencies are almost unchanged by the curvature. In Fig. 2, the relative difference between S_1S_2 ZGV frequencies for the tube and for the plate was plotted as a function of the ratio b/d . In our case of study: A Zircaloy tube with $b = 4.75$ mm and $d = 0.57$ mm ($b/d = 8.33$), the relative difference is lower than 0.1% for circumferential modes and lower than 0.05% for axial waves. Taking into account the thickness variations and frequency measurement accuracy (0.2%), the curvature does not affect the ZGV resonance frequencies. The proposed ZGV technique is still valid in the case of a thin hollow cylinder.

III. ZGV RESONANCE MEASUREMENTS

In the case of an anisotropic plate, it has been observed that ZGV resonances excited by a line laser source on a silicon wafer depend on the line orientation.¹⁵ We use the same procedure to ascertain that the differences between axial and

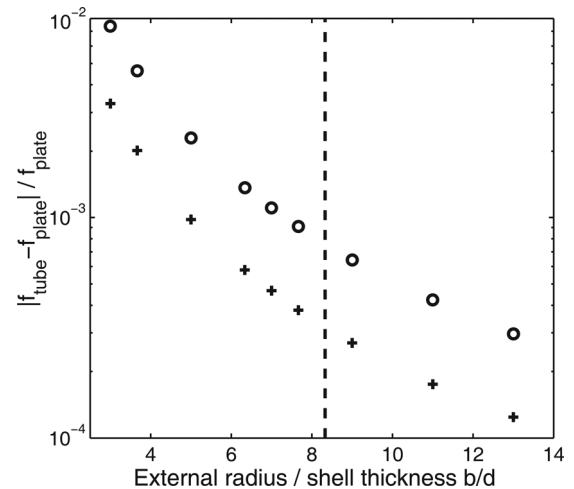


FIG. 2. Relative difference between S_1S_2 ZGV frequencies in a tube and in a plate as a function of the ratio b/d , for circumferential guided waves (\circ) and for axial guided waves ($+$).

circumferential resonances are caused by the material anisotropy and not by the curvature.

As shown in Fig. 3, Lamb waves were generated by a *Q*-switched Nd:YAG (yttrium aluminum garnet) laser providing pulses having a 20 ns duration and 4 mJ of energy. The spot diameter of the unfocused beam is equal to 1 mm. A beam expander ($\times 7.5$) and a cylindrical lens (focal length 250 mm) were used to enlarge the laser beam and focus it into a narrow line on the surface. The optical energy distribution was close to a Gaussian and the absorbed power density was below the ablation threshold. The full length of the source at $1/e$ of the maximum value was found to be 10 mm and the width was estimated to be 0.3 mm. In the thermoelastic regime, the source is equivalent to a set of dipole forces distributed on the surface perpendicular to the line.

Local vibrations were measured by a heterodyne interferometer equipped with a 100 mW frequency doubled Nd:YAG laser (optical wavelength $\Lambda = 532$ nm). This interferometer is sensitive to any phase shift $\Delta\phi$ along the path of the optical probe beam, and then to the mechanical displacement u normal to the surface. As previously shown,²¹ the calibration factor (10 nm/V), deduced from the phase modulation $\Delta\phi = 4\pi u/\Lambda$ of the reflected beam, was constant over the detection bandwidth (500 kHz–20 MHz). Signals detected by the optical probe were fed into a digital sampling oscilloscope and transferred to a computer.

The sample is a hollow cylinder (length 160 mm, external radius 4.75 mm, shell thickness 0.57 mm) made of a zirconium alloy (mass density $\rho = 6.61 \times 10^3$ kg/m³), containing approximately 1.5 wt. % tin, 0.2 wt. % iron, 0.1 wt. % chromium. These Zircaloy tubes are used for cladding fuel rods in nuclear pressurized water reactors. Two measurements were performed at the center of the line, the first one with the source parallel to the cylinder axis [Fig. 4(a)], the other with the source perpendicular to this axis [Fig. 4(b)]. A typical temporal signal is given in Fig. 5. As previously explained, the oscillations in the first 10 μ s are due to the large mechanical displacement associated with the low frequency components of the A_0 Lamb mode.¹⁸ As shown in the insert, the low amplitude tail for $t > 20$ μ s is not noise but high frequency oscillations due to the ZGV resonances.

The spectra of both records are shown in Fig. 6. In the circumferential wave configuration, four resonances appear between 0 and 13 MHz [Fig. 6(a)]. The method exposed in Ref. 14 for an isotropic plate permits to extract the triplet (ν , V_L , V_T) with good accuracy. The uncertainty of the

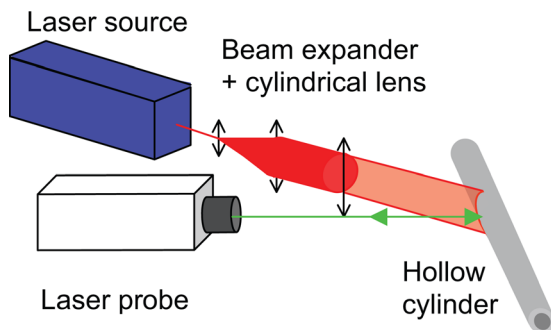


FIG. 3. (Color online) Experimental setup.

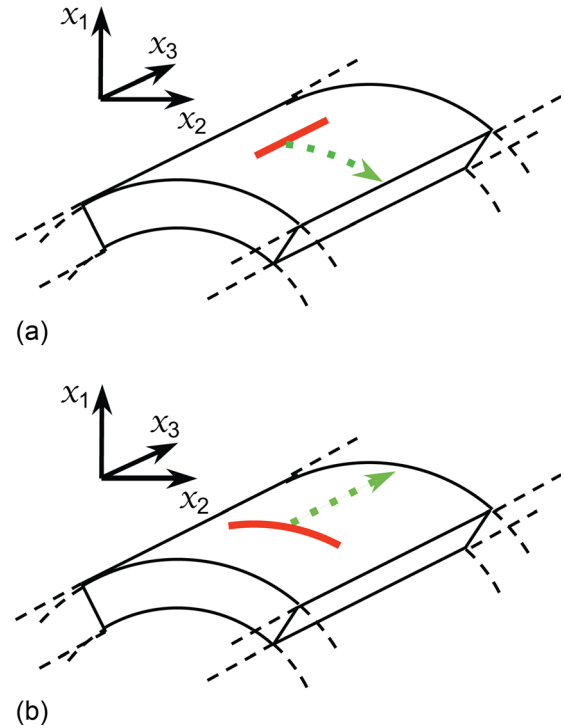


FIG. 4. (Color online) Positions of the line source (a) parallel and (b) perpendicular to the cylinder axis. According to the experiment, the probe laser beam is either at the center or moved perpendicular to the line source.

measurement (0.5% for the Poisson ratio and 1% for the bulk wave velocities) is limited by the quality factor of the resonances (~ 300), the variations of the shell thickness ($\sim 0.1\%$) and the effect of the curvature ($\sim 0.1\%$).

Using the first two resonances, corresponding to the S_1S_2 and A_2A_3 ZGV modes, it was possible to determine $\nu_1 = 0.327$ and then

$$V_{L1} = 4740 \text{ m/s}, \quad V_{T1} = 2405 \text{ m/s}. \quad (1)$$

In the axial wave configuration, only two resonances clearly emerge in the spectrum [Fig. 6(b)], which corresponds to the S_1S_2 and S_3S_6 ZGV modes. A similar method applied to these modes gives $\nu_2 = 0.353$ and

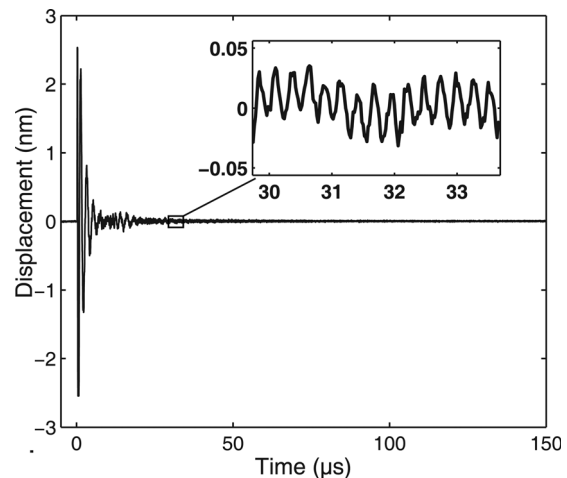


FIG. 5. Normal displacement (nm) recorded at the center of the line source parallel to the cylinder axis.

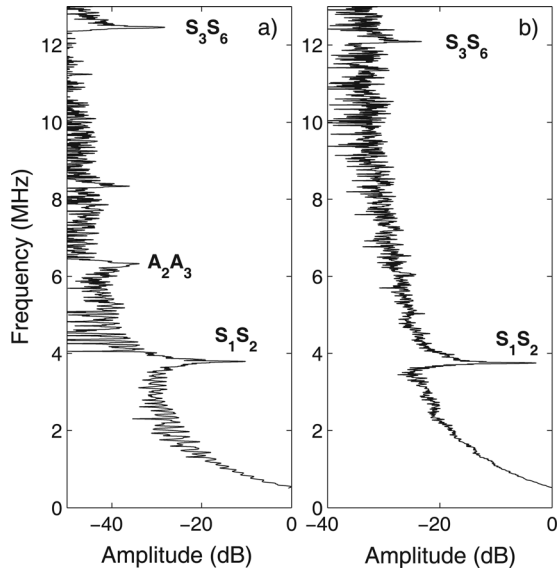


FIG. 6. Spectrum of the resonance for a line source (a) parallel and (b) perpendicular to the cylinder axis.

$$V_{L2} = 4830 \text{ m/s}, \quad V_{T2} = 2300 \text{ m/s}. \quad (2)$$

In conclusion, ZGV measurements and their interpretation in the frame of an isotropic behavior of the material lead to ascribe two relatively different values for Poisson's ratio of the Zirconium alloy. Since this result is not satisfactory, in Sec. IV we develop a transverse isotropic model. The five elastic constants of this model were extracted from ZGV resonances and dispersion spectra of axial and circumferential waves measured with the LBU technique. It should be also noted that the Poisson's ratio ν_2 obtained in the axial wave configuration is very different from that found by Yeh *et al.*¹¹

IV. TRANSVERSE ISOTROPIC MODEL

Given the Cartesian coordinates (x_1, x_2, x_3) with the x_3 -axis parallel to the cylinder axis, the sample is supposed to be isotropic in the (x_1, x_2) -plane. In the linear theory of elasticity, mechanical properties of anisotropic media are described by the stiffness tensor c_{ijkl} . Using the Voigt's notation, they are represented by a 6×6 symmetric matrix $c_{\alpha\beta}$ ($\alpha, \beta = 1-6$). For transverse isotropic media, the number of independent elastic constants reduces to five: $c_{11}, c_{13}, c_{33}, c_{44}$, and c_{66} . Other elastic constants are related to these coefficients or vanish

$$c_{22} = c_{11}, \quad c_{23} = c_{13}, \quad c_{55} = c_{44}, \quad c_{12} = c_{11} - 2c_{66}. \quad (3)$$

The laser beam can be focused along a line parallel or perpendicular to the cylinder axis x_3 (Fig. 4). Assuming the absorbed energy distribution to be symmetric, two waves can be generated by the thermoelastic source with orthogonal polarizations in the sagittal plane perpendicular to the line source at the center.

The classical analysis of elastic wave propagation in a crystal having hexagonal symmetry shows that four phase

velocities are involved.¹⁶ In the first configuration [Fig. 4(a)] and due to the transverse isotropy, the velocities for the two bulk modes are the same, whatever the propagation direction along the surface x_1 or in the shell thickness x_2 :

$$V_{L\perp} = (c_{11}/\rho)^{1/2} \text{ for the longitudinal mode.}$$

$$V_{T\perp} = (c_{66}/\rho)^{1/2} \text{ for the transverse mode whose polarization is perpendicular to the cylinder axis } x_3.$$

In the second configuration [Fig. 4(b)] and due to the anisotropy, the velocities for the longitudinal modes are different:

$$V_{L//} = (c_{33}/\rho)^{1/2} \text{ for the one propagating along the cylinder axis } x_3,$$

$$V_{L\perp} = (c_{11}/\rho)^{1/2} \text{ for the one propagating in the shell thickness } x_2.$$

For the transverse mode, the phase velocity is

$$V_T = (c_{44}/\rho)^{1/2} \text{ whatever the polarization, parallel or perpendicular to the cylinder axis.}$$

Thus, four among the five elastic constants of the transverse isotropic model can be determined from these velocity measurements. Since the thickness is known, velocities can be deduced from ZGV resonance frequencies. In the transverse isotropic case and for a line source parallel to x_3 , circumferential Lamb waves are excited in the transverse isotropic plane and constants c_{11} and c_{66} can be deduced from the extracted velocities $V_{L\perp}$ and $V_{T\perp}$. In the second configuration, axially Lamb waves are generated. The analysis is more complicated since two longitudinal modes are involved, so that the velocity V_{L2} extracted from ZGV resonance frequencies is a combination of $V_{L\perp}$ and $V_{L//}$.

The objective of the following part is to determine the five elastic constants of the transverse isotropic model. For such a number of parameters an inversion process based, for example, on the simplex algorithm is not straightforward. We proposed a simple procedure: Four of the five constants are directly extracted from ZGV resonance frequencies and only the last one c_{13} is deduced from the measured dispersion spectra.

V. RESULTS AND DISCUSSION

It results from the previous analysis that thickness resonance frequencies are independent of c_{13} . They only depend on the four elastic constants c_{11}, c_{66}, c_{33} , and c_{44} . As a consequence, the ZGV resonance frequencies are nearly independent of c_{13} . For example, simulations show that a 10% variation of c_{13} causes only a 0.5% change in the S_1S_2 ZGV resonance frequency. Thus, c_{11}, c_{66}, c_{33} , and c_{44} were determined from ZGV resonance measurements and c_{13} was estimated by fitting theoretical and experimental dispersion curves. Theoretical curves for a transverse isotropic material were calculated with the *Disperse* software.²⁰ Experimental ones were measured with the laser ultrasound setup: The normal displacement was recorded while the probe beam was moved perpendicular to the line source maintained fixed. The fast Fourier transform (FFT) in two dimensions (time and distance) of the obtained B-scans was processed.

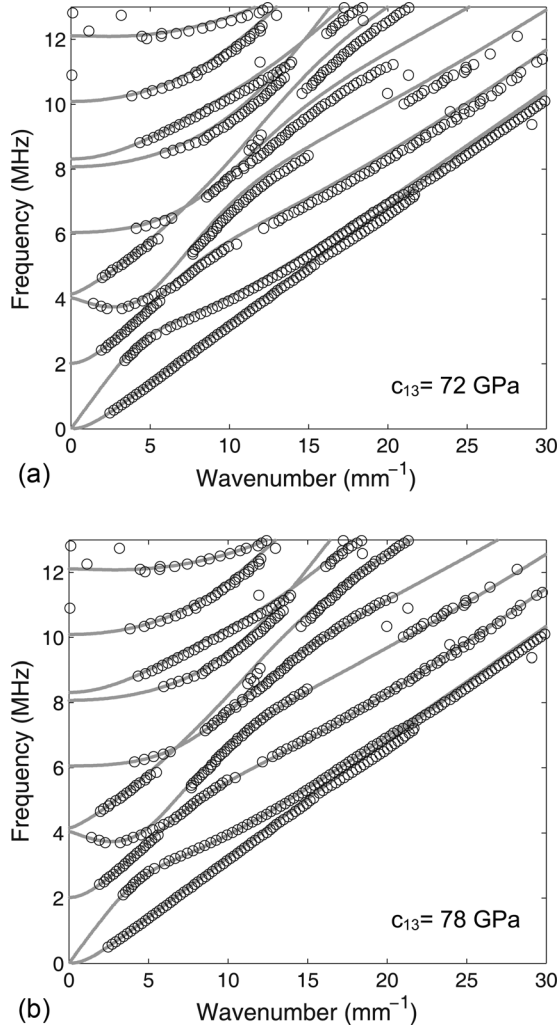


FIG. 7. Transverse isotropic model. Superposition of experimental dispersion curves (○) and calculated ones (gray lines) in the axial direction with (a) $c_{13} = 72$ GPa, (b) $c_{13} = 78$ GPa.

The maxima of the 2D-FFT were extracted to plot the different branches of the dispersion curves in both propagation directions.

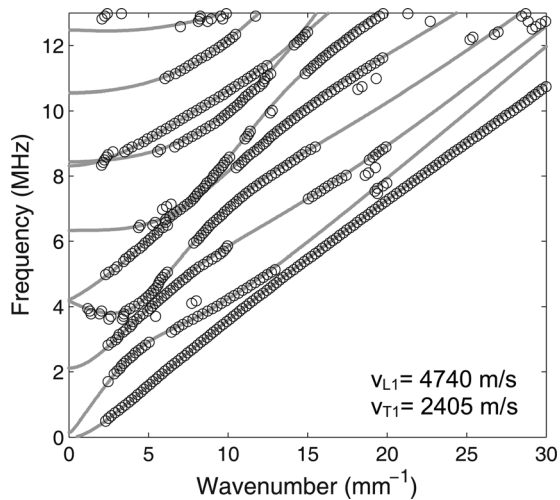


FIG. 8. Superposition of experimental points (○) and dispersion curves (gray lines) calculated for circumferential guided waves.

TABLE I. Stiffness constants in GPa, for the transverse isotropic Zircaloy tube.

c_{11}	c_{12}	c_{33}	c_{13}	c_{44}
149 ± 3	72 ± 2	154 ± 3	78 ± 2	35 ± 1

As the medium is isotropic in the x_1 - x_2 plane, the velocities V_{L1} and V_{T1} obtained in the circumferential configuration [Eq. (1)] are equal to $V_{L\perp}$ and $V_{T\perp}$. Then

$$c_{11} = \rho(V_{L1})^2 = 148 \text{ GPa}, \quad (4)$$

$$c_{66} = \rho(V_{T1})^2 = 38 \text{ GPa}, \quad (5)$$

and

$$c_{12} = c_{11} - 2c_{66} = 72 \text{ GPa}. \quad (6)$$

Constants c_{33} and c_{44} are deduced from ZGV resonance measurements performed in the axial configuration [Eq. (2)]. To simplify the problem, the longitudinal bulk wave velocity $V_{L\parallel}$ is assumed to be equal to the velocity V_{L2} measured by ZGV resonance, so that

$$c_{33} = \rho(V_{L2})^2 = 154 \text{ GPa}. \quad (7)$$

c_{44} is obtained from the transverse bulk wave velocity V_T , equal to V_{T2}

$$c_{44} = \rho(V_{T2})^2 = 35 \text{ GPa}. \quad (8)$$

These values were used as input data for the computation of the dispersion curves of axial guided waves. As in the isotropic case c_{13} and c_{12} are equal, the initial value for c_{13} was chosen as 72 GPa. As shown in Fig. 7(a), the calculated curves are slightly above the experimental ones. A set of dispersion spectra was calculated by varying the value of c_{13} . The best fit was obtained with $c_{13} = 78$ GPa. The corresponding curves drawn in Fig. 7(b) are superimposed on the experimental ones. In the circumferential direction, dispersion curves are identical to those calculated in the isotropic case (Fig. 8). The obtained stiffness tensor constants of the Zircaloy are given in Table I.

VI. CONCLUSION

Elastic guided waves propagating in a Zircaloy hollow cylinder was investigated by LBU techniques. Using a laser line source, ZGV modes were observed in both axial and circumferential configurations. Poisson's ratio values deduced for both configurations from ZGV resonance frequencies differ strongly. It is shown that this difference cannot be ascribed to the geometry of the tube but to the constitutive material. Since the isotropic model was not correct to accurately describe the behavior of guided elastic waves in Zircaloy tubes, a transverse isotropic model was used. Four of the five elastic constants were directly extracted from ZGV resonance frequencies. The last one was deduced from the

dispersion spectra measured by the laser ultrasound technique. A good agreement was obtained between theoretical and experimental dispersion curves for both axially and circumferentially propagating guided waves. In a further study this set of elastic constants can be used as input data for a numerical inversion procedure.

¹P. Gopalan, R. Rajaraman, G. Amarendra, C. S. Sundar, B. Viswanathan, T. Jayakumar, P. Palanichamy, and B. Raj, "Characterisation of β -quenched and thermally aged Zircaloy-2 by positron annihilation, hardness and ultrasonic velocity measurements," *J. Nucl. Mater.* **345**, 162–166 (2005).
²M. P. Gómez, G. Domizzi, M. I. López Pumarega, and J. E. Ruzzante, "Characterization of hydrogen concentration in Zircaloy-4 using ultrasonic techniques," *J. Nucl. Mater.* **353**, 167–176 (2006).
³J. Krautkrämer and K. Krautkrämer, *Ultrasonic Testing of Materials* (Springer, Berlin, 1990), pp. 1–677.
⁴M. J. S. Lowe, D. N. Alleyne, and P. Cawley, "Defect detection in pipes using guided waves," *Ultrasonics* **36**, 147–154 (1998).
⁵Y.-M. Cheong, D.-H. Lee, and H.-K. Jung, "Ultrasonic guided wave parameters for detection of axial cracks in feeder pipes of PHWR nuclear power plants," *Ultrasonics* **42**, 883–888 (2004).
⁶L. C. Lynnworth, *Ultrasonic Measurements for Process Control: Theory, Techniques, Applications* (Academic Press, Boston, 1989), pp. 1–1082.
⁷S. Dixon, C. Edwards, and S. B. Palmer, "High accuracy non-contact ultrasonic thickness gauging of aluminium sheet using electromagnetic acoustic transducers," *Ultrasonics* **39**, 445–453 (2001).
⁸D. W. Schindel, D. S. Forsyth, D. A. Hutchins, and A. Fahr, "Air-coupled ultrasonic NDE of bonded aluminium lap joints," *Ultrasonics* **35**, 1–6 (1997).
⁹C. B. Scruby and L. E. Drain, *Laser Ultrasonics: Techniques and Applications* (Adam Hilger, Bristol, 1990), pp. 1–447.

¹⁰W. Gao, C. Glorieux, and J. Thoen, "Laser ultrasonic study of Lamb waves: determination of the thickness and velocities of a thin plate," *Int. J. Eng. Sci.* **41**, 219–228 (2003).
¹¹C.-H. Yeh and C.-H. Yang, "Characterization of mechanical and geometrical properties of a tube with axial and circumferential guided waves," *Ultrasonics* **51**, 472–479 (2011).
¹²S. Dixon, M. P. Fletcher, and G. Rowlands, "The accuracy of acoustic birefringence shear wave measurements in sheet metal" *J. Appl. Phys.* **104**, 114901 (2008).
¹³S. D. Holland and D. E. Chimenti, "High contrast air-coupled acoustic imaging with zero group velocity Lamb modes," *Appl. Phys. Lett.* **83**, 2704–2706 (2003).
¹⁴D. Clorennec, C. Prada, and D. Royer, "Local and noncontact measurements of bulk acoustic wave velocities in thin isotropic plates and shells using zero-group velocity Lamb modes," *J. Appl. Phys.* **101**, 034908 (2007).
¹⁵C. Prada, D. Clorennec, T. W. Murray, and D. Royer, "Influence of the anisotropy on zero-group velocity Lamb modes," *J. Acoust. Soc. Am.* **126**, 620–625 (2009).
¹⁶D. Royer and E. Dieulesaint, *Elastic Waves in Solids* (Springer, Berlin, 1999), Vol. 1, pp. 1–374.
¹⁷D. Royer, D. Clorennec, and C. Prada, "Lamb mode spectra versus the Poisson ratio in a free isotropic elastic plate," *J. Acoust. Soc. Am.* **125**, 3683–3687 (2009).
¹⁸D. Clorennec, C. Prada, D. Royer, and T. W. Murray, "Laser impulse generation and interferometer detection of zero-group velocity Lamb modes," *Appl. Phys. Lett.* **89**, 024101 (2006).
¹⁹C. Prada, D. Clorennec, and D. Royer, "Local vibration of an elastic plate and zero-group velocity Lamb modes," *J. Acoust. Soc. Am.* **124**, 203–212 (2008).
²⁰B. Pavlakovic and M. Lowe, *Disperse Software, v. 2.0.16* (Mechanical Engineering, Imperial College, London, 2005).
²¹D. Royer and E. Dieulesaint, *Proceedings of the 1986 IEEE Ultrasonics Symposium* (IEEE, New York, 1986), p. 527.